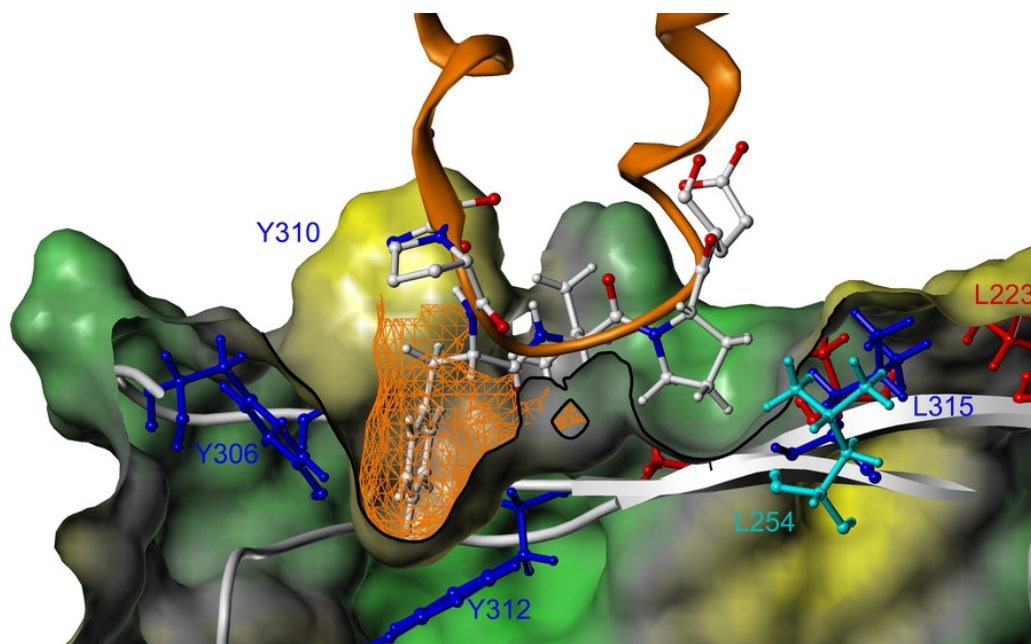
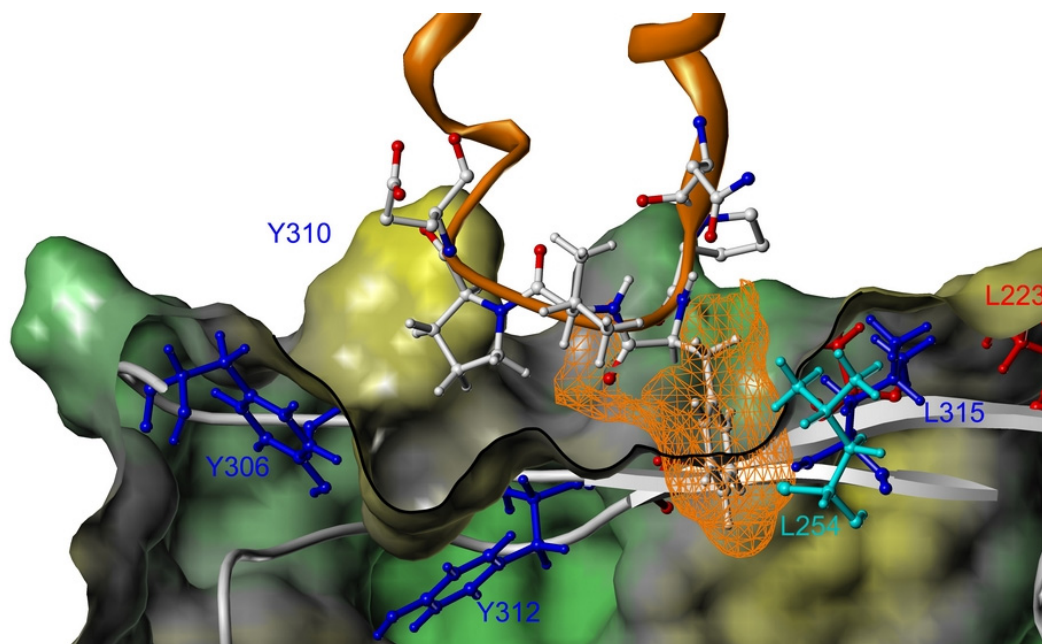
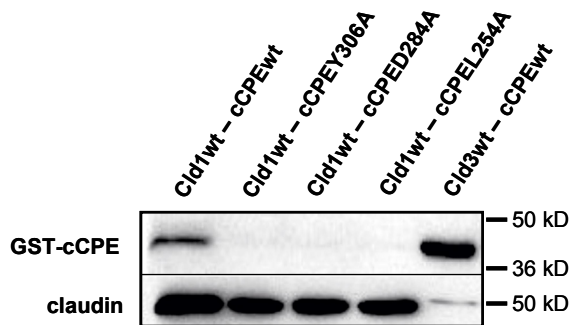
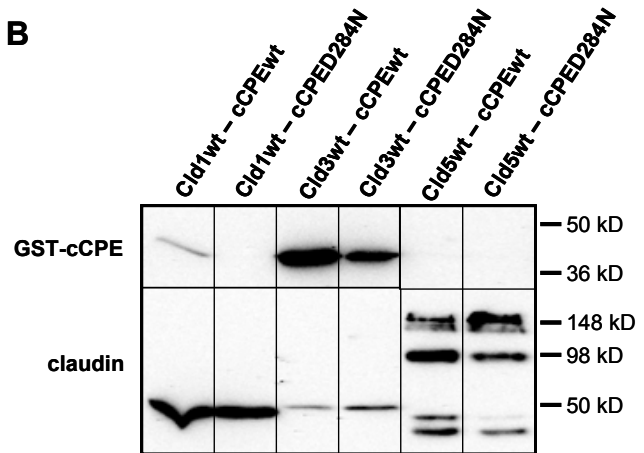


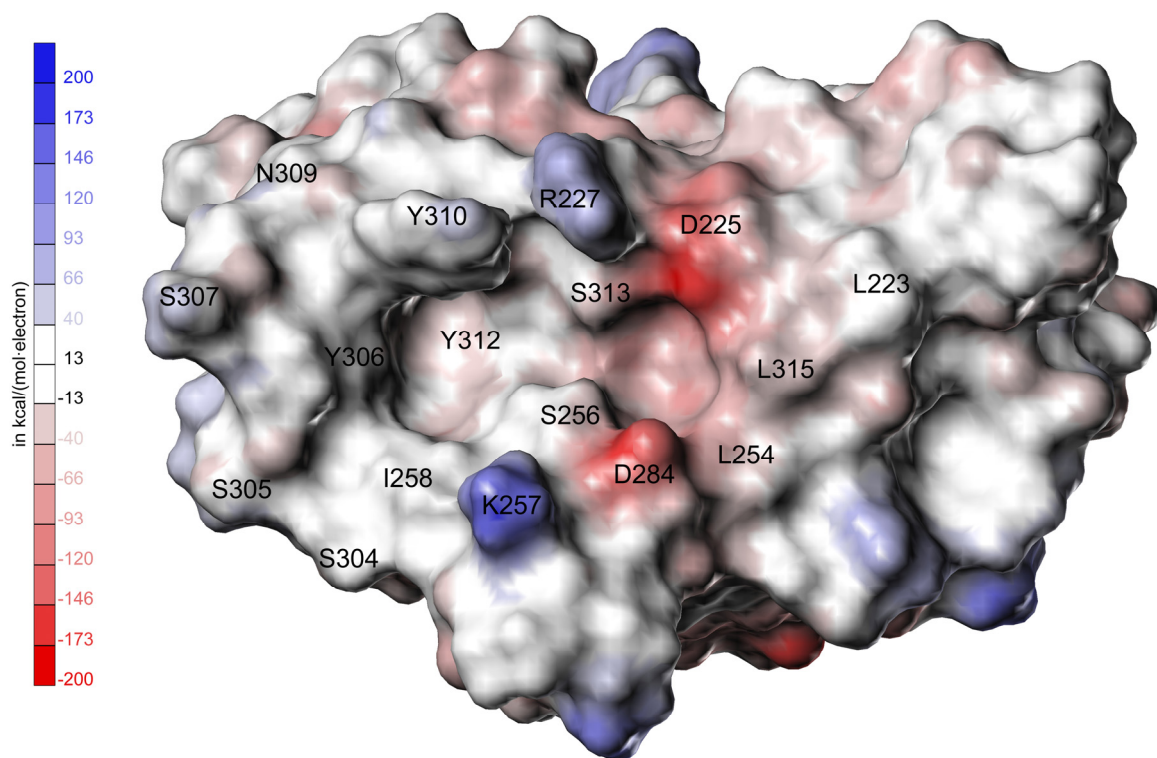
Supplemental figure S1: L151 in ECL2 of Cld4 perfectly fit into the deeper pit of cCPE binding pocket encircled by Y306, Y310 and Y312. Cross section of the interaction model, cCPE shown as cartoon (white) with the surface displayed (green: polar/charged; grey: unpolar; yellow: hydrophobic) and the pocket defining residues in ball and stick (blue: previously described; red: upper rim; cyan: lower rim). Cld4 shown as cartoon (green) with the residues of the turn region as ball and stick (white: C and H; blue: N; red: O) and the surface of L151 (green mesh).

A**B**

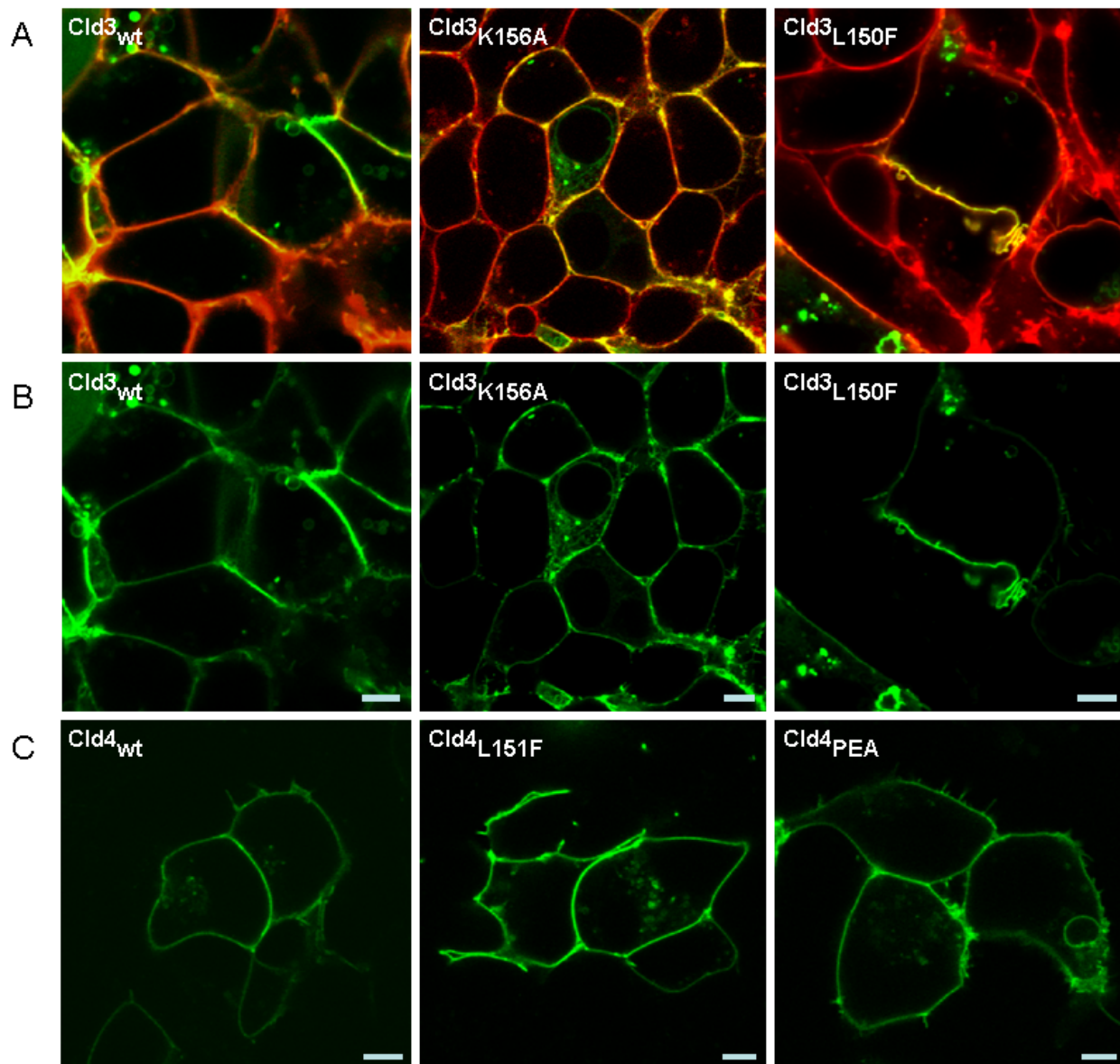
Supplemental figure S2: Cross section of the interaction model for Cld3_{L150F} with cCPE_{wt}. cCPE shown as cartoon (white) with the surface displayed (green: polar/charged; grey: unpolar; yellow: hydrophobic) and the pocket defining residues in ball and stick (blue: previously described; red: upper rim; cyan: lower rim). Cld3 shown as cartoon (orange) with the residues of the turn region as ball and stick (white: C and H; blue: N; red: O) and the surface of F150 (orange mesh). (A) Binding mode of cCPE to Cld3_{L150F} where the Phe is placed in the triple Tyr pit. In (B) it is clear that cCPE can not bind to Cld3_{L150F} in this orientation since the triple Leu pit is not deep enough to accommodate the Phe. Cld3_{L150F} clashes severely with the backbone of the β -sheet (313-319) of cCPE.

A**B**

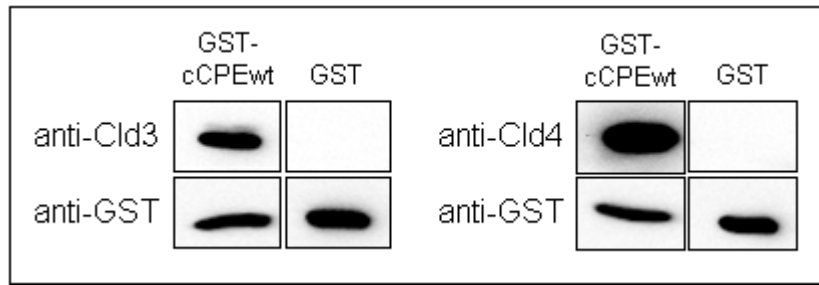
Supplemental figure S3: Substitutions in cCPE do not increase the binding to Cld5 or Cld1. In contrast, they block the weak binding to Cld1 in a similar manner as they block binding to Cld3_{N148D} (Fig. 5C). HEK cells transfected with Cld1_{wt}-YFP, Cld3_{wt}-YFP or Cld5_{wt}-YFP were incubated with 0.5 μ g/ml GST-cCPE_{wt} or mutants thereof. (A, B) Bound GST-cCPE was detected by Western Blots. Representative blots for the cellular binding assay show that Cld1 interacts with cCPE_{wt} more weakly than Cld3 does; note: Cld1 expression detected with anti-GFP antibodies is stronger than Cld3 expression. (A) The substitutions L254A, D284A and Y306A in cCPE blocked interaction with Cld1. (B) Cld5 does not interact with the cCPE_{wt} construct used in this study. Substitution D284N in cCPE decreased the binding to Cld3 and did not enhance the interaction with Cld1 or Cld5. For Cld5, bands for monomers and SDS-resistant multimers were detected, as reported previously (1,2).



Supplemental figure S4: Electrostatic potential map for the binding pocket region of cCPE. The electrostatic potential for the molecular surface was calculated based on Pullman charges, red: areas of low electrostatic potential (negative charge); blue: areas of high electrostatic potential (positive charge).



Supplemental figure S5: Cld3_{K156A}, Cld3_{L150F}, Cld4_{L151F} and Cld4_{PEA} (A153P/S154E/G155A) localize to the plasma membrane similar as the corresponding wild types. This indicates that the amino acid substitutions in the ECL2 do not lead to misfolding of the protein. In contrast, other substitutions in claudins lead to accumulation of the protein in the endoplasmic reticulum indicating misfolding (3). The plasma membrane of living HEK cells was labelled with CellMaskTM Deep Red (Invitrogen, 1.5 μg/ml, 20 min) 3 days after transfection and the subcellular distribution of the claudin construct was analyzed by confocal microscopy. (A) Merge, plasma membrane (red) and claudin-YFP (green); (B, C) claudin-YFP (green); bar, 5 μm.



Supplemental figure S6: GST-cCPE_{wt} but not GST interacts with Cld3 and Cld4 of MDCKI cells. Pull-down assay with lysates of MDCK I cells was performed as described for HEK cells and the eluate was analyzed by Western Blot.

	pI ECL2	Cldwt vs mutant	CPEwt	upper rim				lower rim						triple Y pit			
				L223A	D225A	R227A	LDR	L254A	S256A	K257A	I258A	D284A	D284N	LSI	LSID	Y306A	
Cld4 wt	6.75	+++(+)	+++	++	+++	+	+(+)	++(+)	+++	+++	+++	+++	+++	+++	++(+)	++(+)	+
Cld4 PEA	5.45	+++	+++			+(+)	++(+)								++(+)	++(+)	
Cld3 wt	6.18	+++	+++	++	+++	+(+)	++(+)	+(+)	+++	++(+)	++(+)	++	++	++(+)	(+)		+
Cld3 N148D	4.78	+(+)	+++					-				-	-	-			-
Cld3 L150A	6.18	+(+)	+++														+
Cld3 L150F	6.18	+++	+++				++	+(+)							++(+)		++(+)
Cld4 L150F	6.75	+++	+++				+(+)					++(+)					++(+)
Cld3 E153V	8.59	+++	+++									++		++(+)			(+)
Cld3 Q155E	4.87	+++	+++									++	++	++(+)			+
Cld3 K156A	4.68	+++	+++									++(+)		++(+)			+
Cld3 R157Y	4.68	+++	+++									++(+)		++(+)			+
Cld1 wt	4.68	+	+++					-									-
Cld5 wt	4.68	-															

Table S1: Schematic overview of all binding results between claudin- and cCPE-constructs. Rows: claudins. Columns: cCPE; red, upper rim; blue, lower rim; dark blue, described previously. Extent of binding: no (-), very weak (+), weak (++) to strong (+++). Effect of substitutions in claudins (column: Cld_{wt} vs mutants): Inhibition of cCPE-binding by substitutions in claudins is highlighted in blue. For analysis of substitutions in cCPE, binding of cCPE_{wt} to the respective claudin construct was set as +++ (column: CPE_{wt}): Inhibition of Cld-binding by substitutions in cCPE is highlighted in red; additive effect of substitutions in cCPE and claudins highlighted with orange background; rescue of binding by substitution in claudin highlighted with green background. pI values of the sequences corresponding to mouse Cld3₁₄₀₋₁₆₁. LDR, L223A/D225A/R227A; LSI, L254A/S256A/I258A; LSID, L254A/S256A/I258A/D284A.

Comment: Use of GST-fusion proteins

N-terminal GST-tag was used because it allows efficient purification and detection, shows no relevant unspecific binding (1), and it is a placeholder for an effector domain that might be

used in future applications (4). Furthermore, N-terminal globular domains are connected to cCPE in CPE (5) demonstrating that globular N-terminal domains do not interfere with claudin-binding. However, to minimize any potential effect of the tag, his- or STREP-tag might be considered as an alternative.

Reference List

1. Winkler, L., Gehring, C., Wenzel, A., Muller, S. L., Piehl, C., Krause, G., Blasig, I. E., and Piontek, J. (2009) *J. Biol. Chem.* **284**, 18863-18872
2. Coyne, C. B., Gambling, T. M., Boucher, R. C., Carson, J. L., and Johnson, L. G. (2003) *Am. J. Physiol Lung Cell Mol. Physiol* **285**, L1166-L1178
3. Piontek, J., Winkler, L., Wolburg, H., Muller, S. L., Zuleger, N., Piehl, C., Wiesner, B., Krause, G., and Blasig, I. E. (2008) *FASEB J.* **22**, 146-158
4. Saeki, R., Kondoh, M., Kakutani, H., Tsunoda, S., Mochizuki, Y., Hamakubo, T., Tsutsumi, Y., Horiguchi, Y., and Yagi, K. (2009) *Molecular Pharmacology* **76**, 918-926
5. Kitadokoro, K., Nishimura, K., Kamitani, S., Fukui-Miyazaki, A., Toshima, H., Abe, H., Kamata, Y., Sugita-Konishi, Y., Yamamoto, S., Karatani, H., and Horiguchi, Y. (2011) *J. Biol. Chem.* **286**, 19549-55